

ISSI Visiting Scientists Programme

THE RHESSI MISSION: X-RAY SPECTRA AND IMAGE ANALYSIS BY MEANS OF INVERSION METHODS.

Team Leader: Anna Maria Massone
(CNR-INFN LAMIA, Genova, Italy)

Report of the Third Group Meeting:
September 14-20, 2006

IMAGING AND VISIBILITIES

This meeting was mainly devoted to the understanding of the RHESSI imaging concept [1] and how counts are converted to visibilities.

Image formation: count rate profiles. RHESSI is designed to view the Sun through matched sets of grids. The grid pairs are coaligned so that they modulate the X-rays from a source that is off center from the axis of symmetry. The entire spacecraft is rotated so that the metal bars called *slats* block the source and then the openings called *slits* allow the source to shine on the detector. This means that the detector sees a brightening and darkening source in a regular pattern.

We want first to understand how the rotation of a couple of grids modulates the photon flux coming from a point source located in a certain place in the Sun. For this reason, we try to deduce the analytical expression of the effective area which comes from the superposition of the pair of grids of a single subcollimator.

In general, if $q \in [0, 1]$ denotes the ratio between the width of a slit and the pitch (i.e., the sum p of the width of a slit and the width of a slat) of the subcollimator's grids, it can be shown that the equation which gives the effective area due to the superposition of the grids is given by

$$(1) \quad S(\Phi) = A \left(\frac{c_0}{2} + c_1 \cos(\Phi) + c_2 \cos(2\Phi) + c_3 \cos(3\Phi) + \dots \right),$$

where $\Phi = 2\pi L\theta/p$, L is the distance between the front and the rear grids, θ is the incidence angle between the photon flux and the front grid in 'spatial' units of $p/2L$ and $Ac_0/2$ is the effective area averaged on Φ (in the ideal case of equal slats and slits the averaged effective

area is $A/4$ corresponding to the 25% of the total area). The Fourier coefficients c_k ($k \in \mathbb{N}$) can be calculated starting from the analytic expression of the transmission probability function of the pair of grids (see Figure 1) which is given by:

$$(2) \quad P(\theta) = \begin{cases} 0 & \text{if } -1 \leq \theta \leq -2q \\ \frac{1}{2}\theta + q & \text{if } -2q \leq \theta \leq 0 \\ -\frac{1}{2}\theta + q & \text{if } 0 \leq \theta \leq 2q \\ 0 & \text{if } 2q \leq \theta \leq 1 \end{cases}$$

for $q \in [0, \frac{1}{2}]$ and by

$$(3) \quad P(\theta) = \begin{cases} 2q - 1 & \text{if } -1 \leq \theta \leq -2(1 - q) \\ \frac{1}{2}\theta + q & \text{if } -2(1 - q) \leq \theta \leq 0 \\ -\frac{1}{2}\theta + q & \text{if } 0 \leq \theta \leq 2(1 - q) \\ 2q - 1 & \text{if } 2(1 - q) \leq \theta \leq 1 \end{cases}$$

for $q \in [\frac{1}{2}, 1]$. In these expressions the angle θ is given in units of $p/2L$ and consequently $P(\theta)$, which should be periodic with period p/L in the interval $[-p/2L, p/2L]$, becomes periodic with period 2 in the interval $[-1, 1]$. We can calculate the Fourier coefficients of $P(\theta)$ straightly from their definition:

$$(4) \quad c_0 = \int_{-1}^1 P(\theta) d\theta = 2q^2,$$

$$(5) \quad c_k = \int_{-1}^1 P(\theta) \cos(k\pi\theta) d\theta = \frac{2 \sin^2(k\pi q)}{(k\pi)^2}, \quad k \in \mathbb{Z}_+.$$

Now that we have calculated the effective area of a subcollimator's pair of grids, we can use this expression in order to derive the modulation of the photon flux coming from a point source in the Sun. The photon flux F_0 coming from a point source will be proportional to the effective area of the detector and consequently will be given by

$$(6) \quad C(\Phi) = F_0 T \tau (1 + a_1 \cos(\Phi) + a_2 \cos(2(\Phi)) + a_3 \cos(3(\Phi)) + \dots),$$

where T is the averaged transmission of the detector ($c_0/2$ in the case of a pair of identical grids with a given q), τ is the livetime of the detector and $a_k = \frac{\lambda_k c_k}{T}$, $k \in \mathbb{Z}_+$ (the multiplicative constants λ_k keep into account many physical and technical properties of the subcollimator).

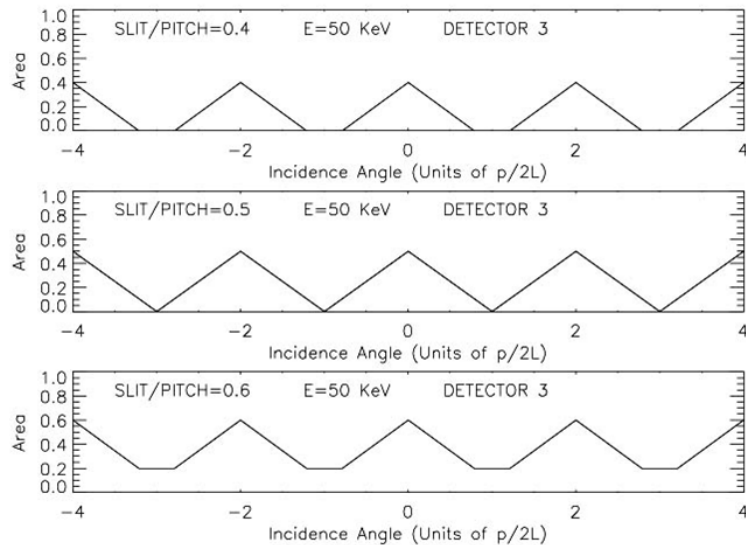


FIGURE 1. Effective area as a function of the incidence angle θ for $q = 0.4, 0.5, 0.6$.

Data stacking. Now we have in our hands the analytical expression of the modulation of a photon flux carried out by a pair of grids of a single subcollimator of RHESSI. What we want to do now is to build an image of the portion of the Sun we are interested in. In order to do this, we have to understand first how RHESSI works and so we have to speak about “data stacking”.

The process of data stacking is something that allows us to consider data coming from multiple rotations equivalent to data coming from a single rotation. This process consists in combining the data on the basis of spacecraft *roll angle* and *aspect phase*. Let us imagine to look at the Sun from the detector’s point of view. At a given instant, the pair of grids will be placed in a certain way and from the detector a certain effective area will be visible.

Let us graph schematically this configuration by displaying the segments in which the transmission is maximum, which essentially correspond to the peaks of the profiles which we have seen for example in Figure 1.

Let us fix now an arbitrary point on the detector and let us denote with I its orthogonal projection on the plane of the image. We denote with (x_{coll}, y_{coll}) the coordinates of I with respect to a fixed coordinate system on the Sun whose axes will be denoted by X_{Sun}, Y_{Sun} . We have to fix a map center M on the Sun with coordinates (x_{map}, y_{map}) with

respect to the same coordinate system and we have to fix the dimensions and the number of the pixels of the map. Let us denote with \mathbf{r}_0 the vector which connects I with M .

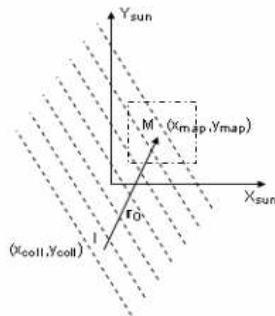


FIGURE 2. The coordinate system fixed on the Sun.

We notice that at each instant we know the coordinates (x_{map}, y_{map}) , which never change in the coordinate system fixed on the Sun, and (x_{coll}, y_{coll}) , which are fixed if we assume that the spin axis of the spacecraft is equal to the axis passing for I while change in a predictable way if the spin axis of the spacecraft is not equal to the axis passing for I . At each instant then we are able to calculate the vector \mathbf{r}_0 . Each pixel l of the image will have coordinates (x_l, y_l) and will be connected with the map center through a vector \mathbf{r}_l .

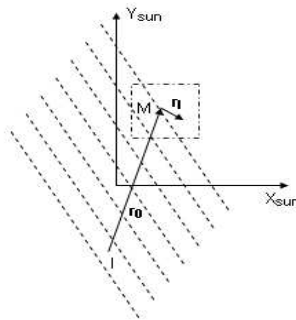


FIGURE 3. The vectors \mathbf{r}_0 and \mathbf{r}_l .

Suppose now that we have a point source located in the pixel l of the map. We observe that the modulation of the photon flux coming from the point source will depend just on the component of \mathbf{r}_0 orthogonal to the slats. We define then a unit vector $\mathbf{k} = (\cos(\alpha), \sin(\alpha))$, where α is the *roll angle* and is equal to the angle made by the axis X_{Sun} and the direction orthogonal to the slats.

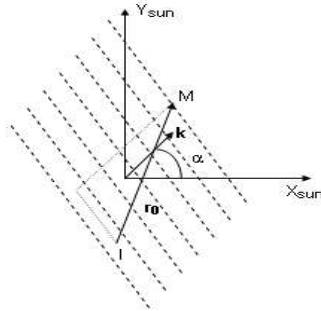


FIGURE 4. The unit vector \mathbf{k} and the roll angle α .

What we called *aspect phase* before is essentially the component of the pointing direction orthogonal to the grid slits and will be proportional to

$$\begin{aligned}
 \mathbf{r}_0 \cdot \mathbf{k} &= (x_{map} - x_{coll}, y_{map} - y_{coll}) \cdot (\cos(\alpha), \sin(\alpha)) \\
 (7) \quad &= (x_{map} - x_{coll}) \cos(\alpha) + (y_{map} - y_{coll}) \sin(\alpha).
 \end{aligned}$$

Let see what does ‘proportional’ means. In the profile vision we have a distance θ (or an angle, if we assume $\theta \approx \tan(\theta)$) which lies in the intervals $[-p/2L + kp/L, p/2L + kp/L]$ and, in order to avoid constants in the expansion of S , we introduce the angle Φ which is proportional to θ and which lies in the intervals $[-\pi + 2k\pi, \pi + 2k\pi]$. When we say “ Φ lies in the intervals $[-\pi + 2k\pi, \pi + 2k\pi]$ ” we mean that the function S seen as a function of Φ is periodic with period 2π , has minimum values in $-\pi + 2k\pi$ and $\pi + 2k\pi$ and maximum values in $0 + 2k\pi$. In the ‘detector’ vision we have again a distance ($\mathbf{r}_0 \cdot \mathbf{k}$) which lies in the interval $[-p/2 + kp, p/2 + kp]$ and again we introduce the proportional angle $\Phi := 2\pi \mathbf{r}_0 \cdot \mathbf{k} / p$ so that Φ still lies in the intervals $[-\pi + 2k\pi, \pi + 2k\pi]$. For this reason the modulation profile seen as a function of Φ is the same as in equation (6) and is given by

$$(8) \quad C(\Phi) = F_0 T \tau (1 + a_1 \cos(\Phi) + a_2 \cos(2(\Phi)) + a_3 \cos(3(\Phi)) + \dots).$$

RHESSI counts are binned into a large number of very short time bins. The top panel of figure 11 shows typical observed counts for a single subcollimator binned into 16 ms time bins and shown for 2 minutes, 4 seconds and 0.4 seconds interval.

Each time bin is associated with the roll angle and aspect phase as we can see in the bottom panel in a roll/phase diagram. The sequence of roll/phase points for a single rotation (4 s) is shown in the top panel of figure 5. Inclusion of many rotations provides a much more

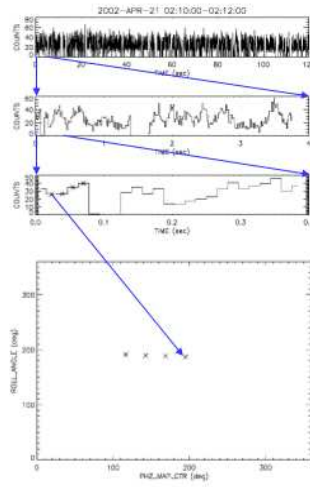


FIGURE 5. RHESSI counts vs time bins.

complete set of roll/phase points (bottom panel of figure 6). This is due to random variations in spacecraft pointing.

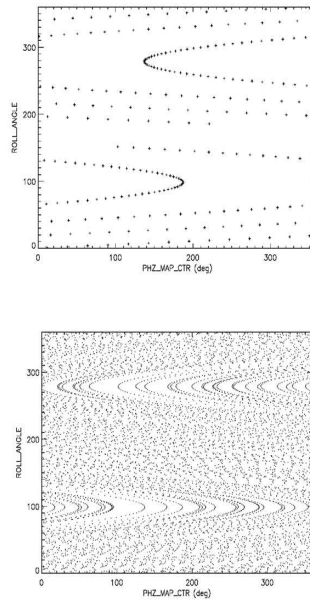


FIGURE 6. Roll/phase diagram for a single rotation and for multiple rotations.

Now roll/phase points are grouped into $M \times N$ roll/phase bins (typically into 32×12 roll/phase bins, but it depends on the user) as we can see in figure 7.

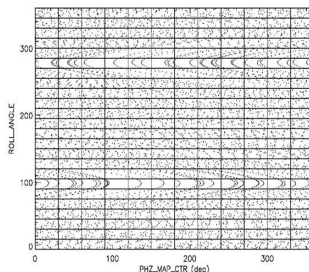


FIGURE 7. The roll/phase bins.

For each subcollimator, if we fix one of the M roll angles, we have the stacked counts as a function of the aspect phase which should theoretically follow the analytical expression given in equation (8) (see figure 8).

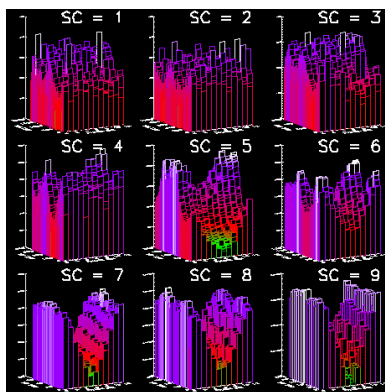


FIGURE 8. Typical plot of count rates as a function of roll/phase bin for all 9 subcollimators.

Visibilities. A visibility is the value of the two-dimensional Fourier transform of a spatial flux distribution $F(x, y)$ at a point in Fourier space:

$$(9) \quad V(u, v) = \iint F(x, y) e^{i\Phi'(x, y; u, v)} dx dy.$$

In the case of a point source placed in the point (x_{map}, y_{map}) of the image, we have

$$(10) \quad F(x, y) = F_0 \delta(x - x_{map}, y - y_{map})$$

and consequently

$$(11) \quad V(u, v) = F_0 e^{i\Phi'}$$

where $\Phi' = 2\pi(ux_{map} + vy_{map}) = 2\pi(x_{map} \cos(\alpha) + y_{map} \sin(\alpha))/p$ (we defined $(u, v) = (\cos(\alpha)/p, \sin(\alpha)/p)$).

The angle Φ' of the visibilities and the angle Φ of the images are strictly related one to the other. We observe from the definition of visibility that Φ' does not depend on the subcollimator coordinates (x_{coll}, y_{coll}) , while this information is certainly and necessary contained in Φ . So if we define the angle $\Delta\Phi = 2\pi(x_{coll} \cos(\alpha) + y_{coll} \sin(\alpha))/p$ we can write the relation

$$(12) \quad \Phi' = \Phi + \Delta\Phi.$$

From equation (8) we have that

$$(13) \quad \begin{aligned} C(\Phi) &= F_0 T \tau (1 + a_1 \cos(\Phi) + \dots) = F_0 T \tau (1 + a_1 \cos(\Phi' - \Delta\Phi) + \dots) \\ &= F_0 T \tau (1 + a_1 \cos(\Phi') \cos(\Delta\Phi) + a_1 \sin(\Phi') \sin(\Delta\Phi) + \dots) \\ &= F_0 T \tau + F_0 T \tau a_1 \cos(\Phi') \cos(\Delta\Phi) + F_0 T \tau a_1 \sin(\Phi') \sin(\Delta\Phi) + \dots \end{aligned}$$

If we neglect the higher harmonics and we fit $C(\Phi)$ with a function like $A \cos(\Delta\Phi) + B \sin(\Delta\Phi) + D$ we obtain

$$(14) \quad A = F_0 T \tau a_1 \cos(\Phi'), \quad B = F_0 T \tau a_1 \sin(\Phi'), \quad D = F_0 T \tau.$$

We observe now that

$$(15) \quad V = F_0 e^{i\Phi'} = F_0 e^{i\Phi + \Delta\Phi} \Rightarrow V e^{-i\Delta\Phi} = F_0 e^{i\Phi} = F_0 (\cos(\Phi) + i \sin(\Phi)).$$

Moreover,

$$(16) \quad \begin{aligned} V e^{-i\Delta\Phi} &= (\text{Re}(V) + i \text{Im}(V)) (\cos(\Delta\Phi) - i \sin(\Delta\Phi)) \\ &= \text{Re}(V) \cos(\Delta\Phi) + \text{Im}(V) \sin(\Delta\Phi) + i (\text{Im}(V) \cos(\Delta\Phi) - \text{Re}(V) \sin(\Delta\Phi)) \end{aligned}$$

and consequently

$$(17) \quad \text{Re}(V e^{-i\Delta\Phi}) = \text{Re}(V) \cos(\Delta\Phi) + \text{Im}(V) \sin(\Delta\Phi).$$

On the other hand, from equations (13) and (15) we have that

$$\begin{aligned}
 \text{Re}(Ve^{-i\Delta\Phi}) &= F_0 \cos(\Phi) = \frac{C(\Phi) - F_0 T \tau}{a_1 T \tau} \\
 (18) \qquad &= \frac{A \cos(\Delta\Phi) + B \sin(\Delta\Phi)}{a_1 T \tau} \\
 &= \frac{A}{a_1 T \tau} \cos(\Delta\Phi) + \frac{B}{a_1 T \tau} \sin(\Delta\Phi).
 \end{aligned}$$

From equations (17) and (18) it follows that

$$(19) \qquad \text{Re}(V) = \frac{A}{a_1 T \tau}, \quad \text{Im}(V) = \frac{B}{a_1 T \tau}$$

and so we have the visibility $V = \text{Re}(V) + i\text{Im}(V)$.

FROM COUNT IMAGES TO ELECTRON IMAGES

The other main goal of the meeting has been the discussion of a new method for imaging spectroscopy analysis of hard X-ray emission during solar flares. The method avoids the traditional noise-sensitive step of stacking independent images made in different count-based energy intervals. Rather, it involves regularized inversion of the count visibility spectra (i.e., the two-dimensional spatial Fourier transforms of the spectral image) to obtain smoothed (regularized) forms of the corresponding electron visibility spectra. Application of conventional visibility-based imaging algorithms then yields images of the electron flux that vary smoothly with energy. During the meeting a first version of the paper concerning this new approach to imaging spectroscopy has been written.

REFERENCES

- [1] Hurford, G. J. et al., 2002, *Solar Phys.*, **210**, 61.